An experimental study of the photodegradation of polyoxymethylene at 122, 147 and 193 nm

Hervé Cottin*, Marie-Claire Gazeau, Jean-François Doussin, François Raulin

*Laboratoire Interuniversitaire des Systèmes Atmosphériques (LISA), UMR 7583 CNRS, Université Paris 7 and Paris 12,
C.M.C., 61 Avenue du Général de Gaulle, 94010 Créteil Cedex, France*

Abstract

This paper presents results from a current experimental program whose aim is to determine quantitatively the photochemical evolution of organic molecules present or likely to be present in comets. Particularly, this includes the mechanisms involved in the degradation of high molecular weight compounds in cometary ices and dust, when they are submitted to photon bombardment in the surrounding area of the sun. Photodegradation of polyoxymethylene $(-CH_2-O-)_n$ is studied at 122, 147 and 193 nm. Experimental setup and analytical methods are presented (FTIR, GC-MS). We have identified the main gaseous photodegradation products of polyoxymethylene: H_2CO, CO, HCOOH, CO_2, CH_3OH, CH_3OCHO, $CH_3OCH_3OCH_3$ and $C_3H_6O_3$ (trioxane). We have determined the production quantum yields for formaldehyde $(\Phi_{122\,nm}=0.75\pm0.21, \Phi_{147\,nm}=0.96\pm0.19)$ and formic acid $(\Phi_{122\,nm}=0.13\pm0.05, \Phi_{147\,nm}=0.26\pm0.10)$, and roughly estimated the yields for the other compounds. Such data, that were missing to interpret astronomical observations of comets, are now available for further theoretical studies. We also propose mechanisms involved in the production of these molecules from polyoxymethylene. © 2000 Elsevier Science S.A. All rights reserved.

Keywords: Polyoxymethylene; UV irradiation; Photodegradation; Experimental design; Quantum yields; Comets

1. Introduction

The degradation of molecules in solid state exposed to energetic photons is complex and far from fully understood. We have developed an experimental set-up designed to study the photodegradation of high molecular weight compounds in the mid and far UV. The aim of our program is to bring a better understanding of the physico-chemical processes involved in the transformation of solid organic materials into smaller gaseous molecules.

Molecules in solid state, especially polymers, can be degraded by energetic radiations. A degradation induced by energetic photons or particles (gamma rays, protons, electrons) with an energy greater than the bond strengths is called *radiolysis*. Far UV photons could be classified in the same category, but their energy is often too low to ionize organic molecules. In this case, one talks about *photodegradation* [1]. Photodegradation processes are strongly depending on experimental conditions: presence or absence of molecular oxygen, nature of chromophores and/or im-

purities which absorb UV photons and induce the degradation. It is initiated by the absorption of a UV photon which leads to a homolysis of the molecule and the production of smaller chains, including gaseous compounds. Such a chemistry results from a competition between initiation, propagation and termination steps of mechanisms involving radicals (see Rabek [2] for a description of polymer photodegradation). The photo-oxidative degradation, i.e. in the presence of molecular oxygen, is rather well documented for many polymers. It has direct applications on the study of materials ageing in the Earths atmosphere. Less is known about photodegradation processes under vacuum, especially in the far UV, whose applications are a matter for space or planetological investigations.

The first molecule that we have studied is Polyoxymethylene (POM: $(-CH_2-O-)_n$) at 122, 147 and 193 nm. This work has been undertaken in the frame of the preparation of the ROSETTA mission (European Space Agency), which will be launched in 2003 to study the gaseous and the solid phase of comet P/Wirtanen in 2010.

Although more than 20 parent molecules have already been detected in the gaseous phase of comets [3] (i.e. stable molecules supposed to come directly from the nucleus, in

* Corresponding author. Fax: +33-1-45-17-15-64.
E-mail address: cottin@lisa.univ-paris12.fr (H. Cottin)

opposition with daughter molecules, which are mainly ions and radicals produced in the cometary atmosphere (called *the coma*) by photodissociation of parent compounds), there is no direct information on the chemical composition of the nucleus. Nevertheless, it is now quite obvious, from observation and laboratory simulations, that the cometary nucleus may contain high molecular weight organics, which cannot be detected by remote sensing spectroscopy, because their vapor pressure is too low for observation techniques, allowing mainly to explore the gaseous phase of the comet (see Cottin [4] for a review on this subject). Only gaseous degradation products of these molecules could be detected by remote observations.

Observations with a high spatial resolution have shown that the density profile in the coma of some compounds is different from the one expected with a molecule directly ejected from the nucleus: in this case, one talks about an *extended source*. This is the case for CO in several comets [5–7] and for the formaldehyde (H_2CO) in comet Halley [8], as well as in comets Hyakutake [9] and Hale–Bopp [10]. Since polyoxymethylene, a polymer of H_2CO, has been tentatively detected in comet Halley [11], and is produced during some laboratory simulations of cometary ices [12], it is often evoked as a parent molecule of formaldehyde to explain that extended source by photo- or thermal degradation [8,13,14]. To date, there was no quantitative study available about the degradation of POM, preventing from any modeling of such a phenomenon to conclude whether POM may be responsible for those unexpected H_2CO density profiles.

Indeed, there are only few data concerning polyoxymethylene degradation in condition relevant to cometary environment. To date, most of the studies are only concerned with photo-oxidative degradation of POM, leading to the production of molecules such as CO, CO_2, HCOOH, CH_4 and C_2H_6 [2]. But chemical mechanisms, products and reaction yields might be very far from what we are expecting without molecular oxygen. According to Rabek [2], photodegradation under vacuum or in an inert atmosphere should only produce H_2CO and some CO. This last molecule being only secondary produced by H_2CO photochemistry. Irradiation of POM under vacuum and for wavelengths below 200 nm have already been reported [15]. This work concludes to the formation of CO and H_2CO in the gas phase (identified by direct MS), while an infrared analysis of the solid irradiated residue reveals the presence of ester functions. This study remains unfortunately qualitative, and has not been followed out to our knowledge. More is known about POM radiolysis. Under vacuum, the polymer irradiated by 1 MeV electrons, produce several gaseous compounds as H_2, CH_4, CO, H_2CO, CH_3CHO, CH_3OCHO, $CH_3OCH_2OCH_3$, CH_3OCH_2OCHO and H_2O. The production yield of formaldehyde from the polymer is $G_{H_2CO}=4\pm1$ [16].

In this paper, we present the experimental development, and the quantitative results we obtained concerning the photodegradation of polyoxymethylene at 122, 147 and 193 nm.

2. Experimental

We have developed a reactor in which solid molecules can be irradiated, at a controlled temperature, in the far UV and in pressure conditions close to the cometary environment. Gaseous molecules produced are analyzed by different and complementary methods: direct mass spectroscopy (MS), infrared spectroscopy (FTIR) and gas chromatography coupled to a mass spectrometer (GC-MS). Our experimental setup (see Fig. 1) is called S.E.M.A.Ph.Or.E. Cométaire (A french acronym: Simulation Expérimentale et Modélisation Appliquées aux PHénomènes ORganiques dans l'Environnement Cométaire).

2.1. Photochemical reactors

Two reactors, made of Pyrex, have been used for our analysis. Both of them are equipped with a vacuum stopcock leading to the analysis system and another connection to a secondary vacuum pump (Turbomolecular pump, Balzers). The pressure is measured in the reactor by a Baratron sensor MKS 627A-01TDC (range, 10^{-4}–1 mb). A vacuum better than 10^{-4} mb can be reached during pumping. One reactor is used for the determination of the lamp flux by chemical actinometry: it is deeper than the second one, and thus allows a longer optical path for the UV to be absorbed by the actinometer gas. The other reactor has a double wall for circulation of a thermostated liquid necessary to operate at a constant temperature.

2.2. Chemical

We have used commercial polyoxymethylene (>99.5%, Prolabo, France). The polymer is deposited at the bottom of the thermostated reactor and irradiated at different wavelengths after several days of pumping. Its temperature is set at 298 K during irradiation.

2.3. Irradiation

The UV irradiation system is composed of a lamp filled with an appropriate gas or gas mixture according to the emitted wavelength: 5.5 mb H_2 (2%) in He (>99.99%, Linde, France) for a 122 nm emission (Lyman α), 0.3 mb Xe (99.99%, Linde, France) for 147 nm, and 0.5 mb CH_4 (1%) in He (>99.99%, Linde, France) for 193 nm. Discharge in the lamp is initiated with a Tesla coil and the gas is excited by a microwave generator (Somelec, France) with a power of 200 W at 2450 MHz. The pressure of the gas in the lamp is set at a level allowing to maintain a stable discharge. Titanium wires heated by an electric current can be used as efficient getters to purify Xenon during 147 nm experiments. In order to perform reproducible experiments, the microwave cavity electrodes are adjusted so that the visible component of the plasma reaches the transmission window
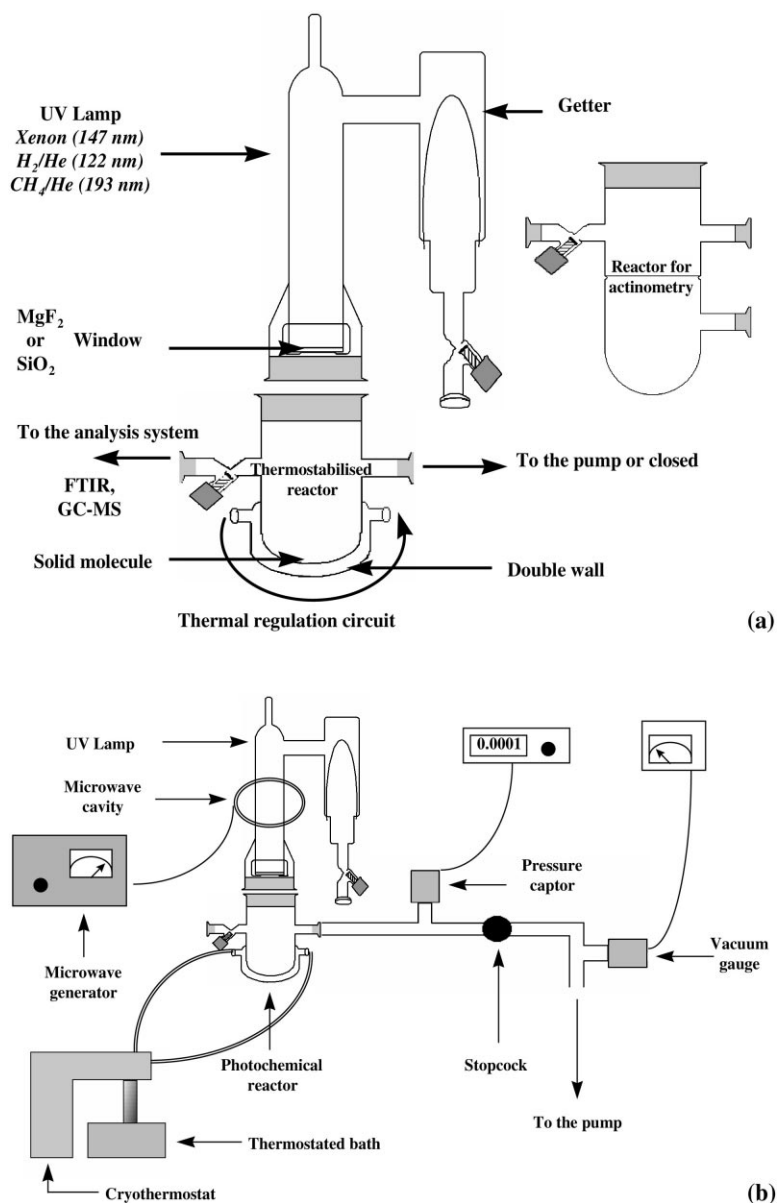
Fig. 1. (a) Photochemical reactors and UV lamp; (b) experimental setup organization.

of the lamp. Two different windows are used: MgF_2 for transmission of 122 and 147 nm UV, and SiO_2 for 193 nm (thickness: 2 mm; Φ: 25 mm, Sorem, France). The SiO_2 window absorbs UV below 170 nm, and thus filters the other atomic lines of C atom at 166 and 156 nm [17]. For each wavelength, the UV lamp flux is measured by chemical actinometry. Actinometers have been chosen to be relevant of the irradiation conditions: significative cross section at the studied wavelength and simple photochemistry. Results are described and discussed in details in Cottin [18].

The Lyman α lamp flux ($\lambda=122$ nm) has been estimated using CO_2 (>99.99%, Linde, France) as an actinometer. The CO production during CO_2 photolysis has been measured with an infrared spectrometer (Perkin-Elmer 1710).

The number of photons emitted by the lamp has then been derived assuming $\Phi_{CO/122\,nm}=1$ for the quantum yield of CO production from CO_2 [19,20]. The UV spectrum of CO_2 used to evaluate the fraction of the lamp flux absorbed by the actinometer is from [17]. We have performed an absolute infrared CO calibration (>99.99%, Air Liquide, France). The value for the lamp flux obtained by this method is $f_{122\,nm}=(2.30\pm0.64)\times10^{15}$ photons s^{-1}.

The Xenon lamp flux ($\lambda=147$ nm) has been estimated using N_2O (99%, Air Liquide, France) by an accurate pressure measurement during its photolysis. From [20,21], the net production of molecules in the 138–210 nm range is $\Phi_{\Delta n}=1$, resulting from a global reaction that could be described by the following expression:

$2N_2O + h\nu \rightarrow (3/2)N_2 + NO + (1/2)O_2$ [17]. The reference UV spectrum that has been used for N_2O is also from [17]. The value $f_{147\,nm} = (1.09 \pm 0.17) \times 10^{16}$ photons s^{-1} has been derived from this actinometry.

The methane lamp flux ($\lambda = 193$ nm) has been estimated using ethylene (99.95%, AGA, France), whose one of the photolysis way at 193 nm is $H_2C=CH_2 + h\nu \rightarrow HC\equiv CH + H_2$. A value of $\Phi_{H_2} = 0.5$ is recommended by [22] after an exhaustive review on this subject. According to the same review, our reference UV spectrum for C_2H_4 is taken from ref [23]. After irradiation, C_2H_4 and C_2H_2 are trapped in liquid nitrogen. Then, total pressure in the reactor gives us the number of molecular hydrogen formed, and thus the number of photons emitted by the lamp and absorbed by the actinometer. For this lamp, $f_{193\,nm} = (1.32 \pm 0.22) \times 10^{15}$ photons s^{-1} has been obtained.

2.4. Analysis

Chemical analysis of the gaseous phase resulting from the irradiation of the solid molecule has been carried out by direct MS, FTIR and GC-MS. Results obtained by direct MS have already been presented and discussed in a previous paper [24]. In order to perform FTIR analysis, the photochemical reactor is connected to a 1 m^3 atmospheric simulation chamber that has been developed in our laboratory [25]. In the case of the S.E.M.A.Ph.Or.E. Cometaire experiment, the gaseous photodegradation products diffuse from the reactor to the chamber, where they can be analyzed thanks to a multireflection infrared analysis system [26] (Bomem DA8-ME: optical path, 12–620 m; range, 600–4000 cm^{-1}; resolution, 64–0.013 cm^{-1}). Prior to an experiment, the interior of the chamber is emptied by pumping up to a vacuum of about 10^{-3} mb. In the same time, the walls of the chamber are heated at about 310 K to make desorption of adsorbed molecules easier. Then, irradiations are performed in an inert atmosphere of 2 mb Helium (>99.99%, Alpha Gaz, France) in order to avoid desorption of molecules remaining after pumping. Identification and quantification of different products are based on our own calibrations, performed at the same total pressure than the one of photodegradation experiments (2 mb He). The spectra of the resulting gaseous phase after POM irradiations have been carried out using an optical pathway of 96 or 288 m, and a resolution of 0.5 cm^{-1}.

The last analysis method used is GC-MS. In this case, preconcentration of the gas sample resulting from irradiations is required to allow the detection of photodegradation products in very low amount. A cold trap (liquid nitrogen) is connected to the reactor where experiments are performed under vacuum (10^{-4} mb at the beginning of the irradiation). At the end of the experiment, the trap is warmed up at room temperature and the resulting gaseous sample is injected into a GC (Varian 3400), through an apolar column (MXT-1/Restek: internal diameter, 0.15 mm; length, 30 m; film thickness, 0.6 μm; head pressure, 15 psi). The detector is a ion trap mass spectrometer (Finnigan-Varian), ranging from 1 to 650 amu, with a resolution of 1 amu. The temperature programming for the column is 273 K: 0–5 min/273 → 333 K: 5–11 min/333 K: 11–20 min. Identification of products is based on both mass spectra and retention time measured after injection of standard compounds.

## 3. Results

3.1. Infrared results

An example of infrared spectrum obtained after a 7 h irradiation of polyoxymethylene at 122 nm is shown on Fig. 2. Several molecules are detected: H_2CO (formaldehyde: signature around 2800 and 1745 cm^{-1}), CO (carbon monoxide: signature between 2200 and 2000 cm^{-1}), CO_2 (carbon dioxide: signature between 2400 and 2200 cm^{-1} and at 614 cm^{-1}), HCOOH (formic acid: PQR signature centered at 1105 cm^{-1}), CH_3OH (methanol: PQR signature centered at 1033 cm^{-1}), CH_3OCHO (methyl formate: signature at 1755 and 1209 cm^{-1}). The same molecules are detected at 147 nm. Irradiations at 193 nm resulted in a very low production of H_2CO along with traces of CO and HCOOH. For this wavelength, thermal degradation of POM seems to be the main observed mechanism because other photodegradation products were not detected (heating POM is the usual way to obtain pure H_2CO because commercial solutions of formaldehyde contain methanol to avoid polymerization of the molecule).

Quantum yields for the production of H_2CO and HCOOH from POM have been calculated, whereas rough estimation have been obtained for CO, CO_2 and CH_3OH. CH_3OCHO is produced in such a small amount that it has not been quantitatively studied.

3.2. H_2CO

3.2.1. 122 nm
Successive spectra have been collected to follow the production rate of formaldehyde. Evolution of its absorbance (1745 cm^{-1}) is shown on Fig. 3. From these quantitative results, it is easy to derive the production rate of this gaseous molecule from the polymer ($V_{H_2CO/122\,nm}$ = number of produced molecules/irradiation time). Nevertheless, rough results have to be corrected because between its emission from the polymer and the moment it enters the connection between the reactor and the atmospheric chamber, a molecule can be photolysed. The possible primary photodissociation processes are [27]
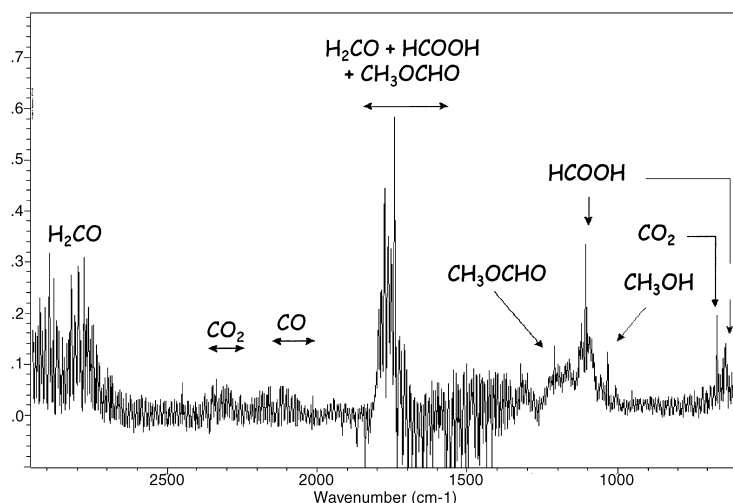
$$H_2CO + h\nu \rightarrow CO + H_2$$

$$H_2CO + h\nu \rightarrow CO + 2H$$

$$H_2CO + h\nu \rightarrow HCO + H$$
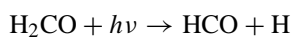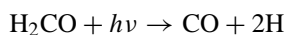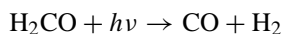
Fig. 2. Infrared spectrum of the gaseous phase after 7 h of POM irradiation at 122 nm. Optical path: 288 m; resolution: 0.5 cm^{-1}; polymer temperature: 298 K.

The photolysis rate is given by

$$\frac{d|H_2CO|}{dt} = -J|H_2CO|$$

with a photolysis constant $J = \int_\lambda \sigma I \Phi \, d\lambda$. Those parameters are function of λ. A monochromatic emission from the lamp is assumed where the cross section for H_2CO at the considered wavelength [27] $\sigma = 1.42 \times 10^{-17}$ cm^2; lamp flux $I = 6.64 \times 10^{14}$ s^{-1} cm^{-2}; dissociation quantum yield, Φ, that we consider as equal to one at this wavelength [27], then $J = 9.43 \times 10^{-3}$ s^{-1}. The amount of H_2CO destroyed is proportional to its residence time (τ) under irradiation in the reactor, $\tau = l/v$ where l is the reactor's length and v the mean compound's speed. If one considers molecular diffusion, $v = F/C$ where F is H_2CO flux (s^{-1} cm^{-2}) and C the concentration (cm^{-3}). F is measured at H_2CO entrance in the simulation chamber, it is constant between the reactor and the chamber apart from connection's section variations. Furthermore the concentration is measured in the simulation chamber. Thus, to estimate v in the reactor, we have to go back to the mean concentration in the reactor using the first Fick's law

$$\frac{\partial C}{\partial z} = -\frac{F}{D}$$

D is the diffusion coefficient of formaldehyde in helium, estimated with the following expression [28]:

$$D_{A/B} = \frac{5.457 \times 10^{17}}{n(s_A + s_B)^2} \times \sqrt{\frac{T(M_A + M_B)}{M_A M_B}}$$

A and B are the two considered molecules, n the total density (cm^{-3}), M the molar mass (g mol^{-1}), s the collision cross section ($s_{He} = 0.255$ nm, $s_{H_2CO} = 0.37$ nm) [29] (estimated for H_2CO). Then $D_{H_2CO/He} \sim 350$ cm^2 s^{-1}. Thus, knowing the geometry of our setup and the different connections, it is possible to estimate $\tau \sim 4$ s, and that the percentage of formaldehyde destroyed ($J\tau$) in the reactor is less than 4%.

The thermal degradation of POM has also to be considered. Indeed, the polymer is in equilibrium with formaldehyde (POM$\Leftrightarrow nH_2CO$) [30]. Production of H_2CO from POM by thermal degradation is very difficult to study quantitatively. Nevertheless, its contribution during irradiations has to be estimated: it depends on the progress
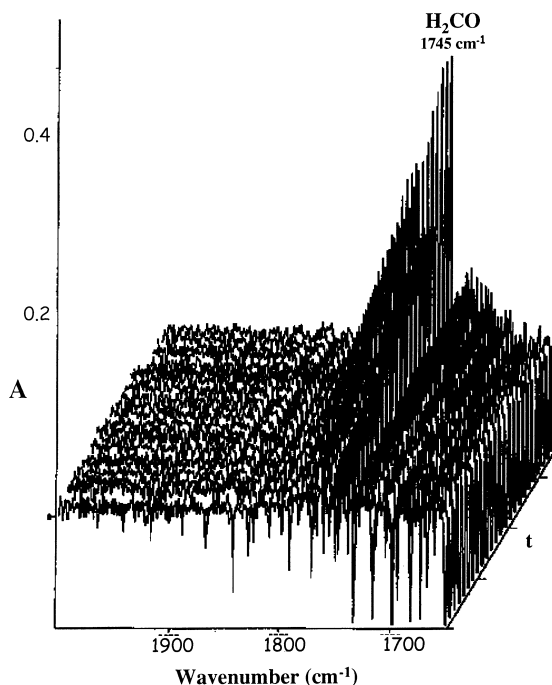

Fig. 3. Formaldehyde appearance in the simulation chamber during UV irradiation of POM. The graph present evolution of the H_2CO signature intensity at 1745 cm^{-1} as a function of time.
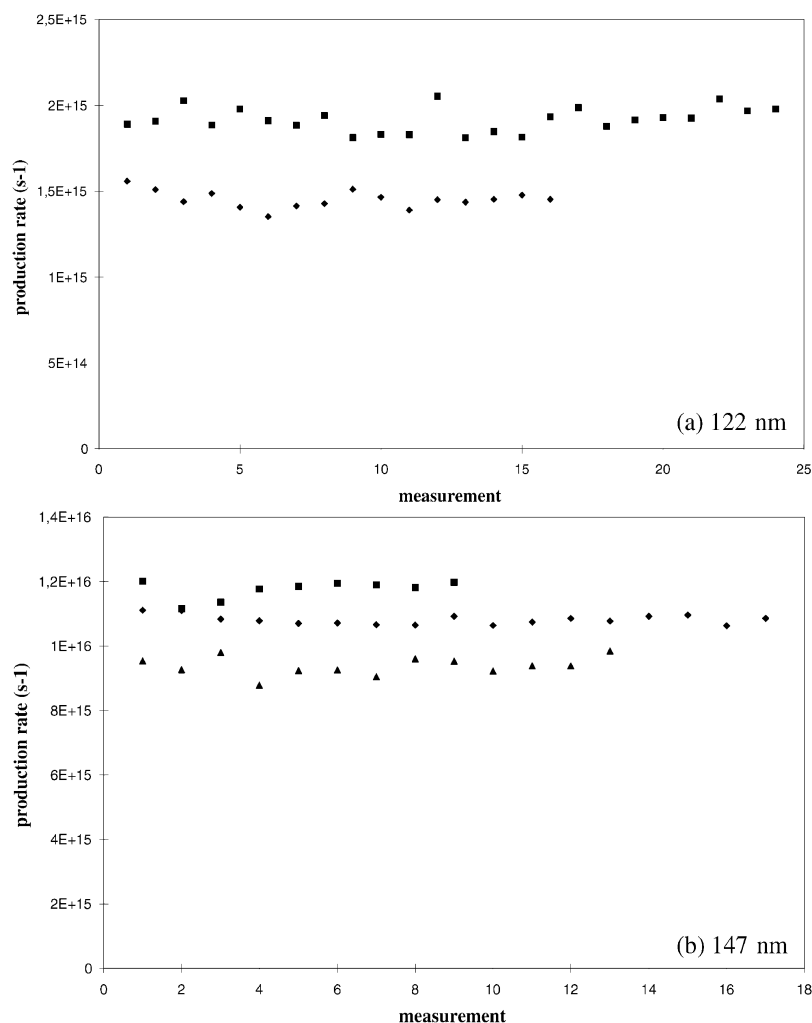
Fig. 4. Production rate of formaldehyde from POM. (a) for two independent irradiation experiments at 122 nm; (b) three independent experiments at 147 nm.

of the equilibrium, if it is studied under vacuum or in an Helium atmosphere, and with or without irradiation. Thus, we have corrected our results by the formaldehyde production at 193 nm for which we have estimated that the photodegradation contribution is negligible compared to the thermal degradation (see Section 3.3.2). As formaldehyde is the only compound produced by thermal degradation of POM, such a correction is useless for the other molecules.

We have performed two independent 122 nm irradiations, and the results, corrected by photochemistry and thermal contribution, are presented on Fig. 4a. Then, the mean production rate derived is $V_{H_2CO/122\,nm}=(1.73\pm0.48)\times 10^{15}\,s^{-1}$. It is likely that the difference between the two independent experiments is due to a variation of the lamp flux. Indeed, such a variation is compatible with variation range of the flux estimated around the nominal value ($f_{122\,nm}=(2.30\pm0.64)\times10^{15}$ photons s^{-1}, i.e. $\pm28\%$). This margin of error is kept to calculate the 122 nm quantum yield of formaldehyde production from polyoxy-

methylene ($V_{H_2CO/122\,nm}/f_{122\,nm}$):

$$Q_{H_2CO/122\,nm} = 0.75 \pm 0.21$$

As expected, formaldehyde production by POM photodegradation is quite efficient. This yield is lower than the value $G_{H_2CO}=4\pm1$ obtained for 1 MeV electrons radiolysis [16], which is consistent with the fact that energetic particles penetrate deeper than UV photons, and are able to break more chemical bonds.

3.3. Influence of the wavelength

3.3.1. 147 nm

Three independent irradiations at 147 nm have also been performed. For these measurements, thermal contribution is negligible compared to photodegradation because of the high flux of the Xenon lamp. Taking into account the formaldehyde photodestruction rate with the following parameters: $\sigma=6.74\times10^{-18}\,cm^2$ [17,27], $I=3.16\times10^{15}\,s^{-1}.cm^{-2}$,

$\Phi=1$, we obtain $J=0.021\,\text{s}^{-1}$. The results are shown on Fig. 4b. We obtain $V_{\text{H}_2\text{CO}/147\,\text{nm}}=(1.06\pm0.21)\times10^{16}\,\text{s}^{-1}$. Again, we can consider that the difference between the independent experiments is a consequence of a variation of the lamp flux in the estimated range around its nominal value ($f_{147\,\text{nm}}=(1.09\pm0.17)\times10^{16}\,\text{photons}\,\text{s}^{-1}$).

$$Q_{\text{H}_2\text{CO}/147\,\text{nm}} = 0.96 \pm 0.19$$

Quantum yields for both wavelengths can be considered as equal within the uncertainty range.

3.3.2. 193 nm

As already mentioned, only formaldehyde is produced in noticeable amount at 193 nm, with traces of carbon monoxide and formic acid. As H_2CO cross section is negligible for this wavelength [17,27], photodestruction of the molecule in the irradiation reactor has not to be considered.

As the C–O bond strength in POM is about $500\,\text{kJ}\,\text{mol}^{-1}$, a photodissociation of the polymer for wavelengths beyond 190–200 nm, could not be envisaged without implication of impurities or photooxidative mechanisms [2]. Considering the small amount of formaldehyde produced at 193 nm, and the absence of other quantifiable photodegradation compounds, we made the hypothesis that thermal degradation is predominant at this wavelength. The formaldehyde production rate at this wavelength has been used to estimate the relative contribution of thermal- and photodegradation at 122 and 147 nm. As H_2CO is the only thermal degradation product of POM, traces of CO and HCOOH are nevertheless indicating that some photodegradation occurs. The production rate derived for 193 nm is an upper limit for the thermal degradation of POM under UV irradiation at 298 K: $V_{\text{H}_2\text{CO}/193\,\text{nm}}=(2.08\pm0.18)\times10^{14}\,\text{s}^{-1}$. On the contrary, if a dominant photodegradation is assumed, an upper limit for the quantum yield can be calculated: $V_{\text{H}_2\text{CO}/193\,\text{nm}}<0.16$.

3.4. Other compounds

3.4.1. HCOOH

HCOOH production has also been studied as a function of the wavelength. Evolution of its PQR signature centered at $1105\,\text{cm}^{-1}$ is shown on Fig. 5. Rough results have to be corrected from photochemistry:
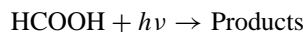
$$\text{HCOOH} + h\nu \rightarrow \text{Products}$$

products are H_2, CO and CO_2 [17] with $\sigma_{122\,\text{nm}}=1.2\times10^{-17}\,\text{cm}^2$, $\sigma_{147\,\text{nm}}=2.1\times10^{-17}\,\text{cm}^2$ [31], $\Phi_{122/147\,\text{nm}}=1$, we calculated $J_{122\,\text{nm}}=8.0\times10^{-3}\,\text{s}^{-1}$ and $J_{147\,\text{nm}}=6.6\times10^{-2}\,\text{s}^{-1}$. On the other hand $s_{\text{HCOOH}}=0.4\,\text{nm}$ is estimated from ref [29]. It allows us to calculate $D_{\text{HCOOH}/\text{He}}\sim314\,\text{cm}^2\,\text{s}^{-1}$ and residence time of formic acid in the reactor: $\tau\sim4\,\text{s}$. Results are shown on Fig. 6 and lead to: $V_{\text{HCOOH}/122\,\text{nm}}=3.06\times10^{14}\pm5.23\times10^{13}\,\text{s}^{-1}$ and $V_{\text{HCOOH}/147\,\text{nm}}=2.84\times10^{15}\pm8.35\times10^{14}\,\text{s}^{-1}$. Relative uncertainty is higher than formaldehyde results. This can be
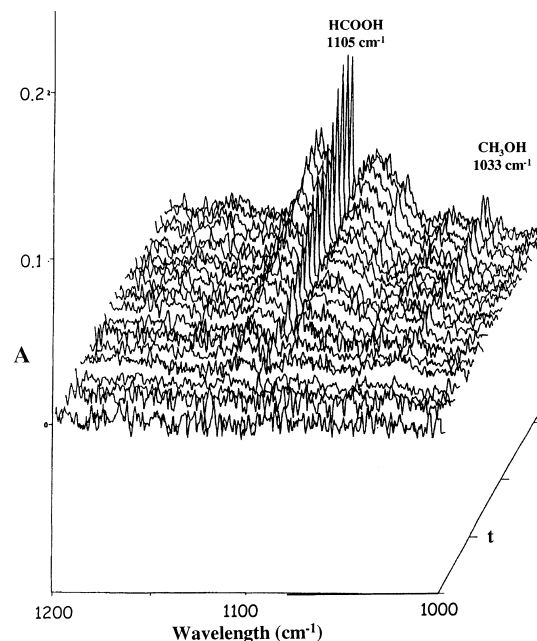

Fig. 5. Formic acid and methanol appearance in the simulation chamber during UV irradiation of POM. The graph present evolution of the HCOOH signature at $1105\,\text{cm}^{-1}$ and the CH_3OH signature at $1033\,\text{cm}^{-1}$ as a function of time.

explained by the low amount of formic acid measured by IRTF and quantified in the lower concentration range of our calibration. For this concentration range, estimated uncertainty is about 40%. Thus, it is this last relative uncertainty that has been kept to estimate quantum yields:

$$Q_{\text{HCOOH}/122\,\text{nm}} = 0.13 \pm 0.05$$

$$Q_{\text{HCOOH}/147\,\text{nm}} = 0.13 \pm 0.10$$

Again, both results can be considered as equal within the uncertainty range. Considering the extremely low amount of HCOOH detected at 193 nm, we just can derive: $Q_{\text{HCOOH}/193\,\text{nm}}=\varepsilon$.

3.4.2. CO

Results concerning CO production are extremely scattered (Fig. 7) because the produced amount is at the level of its detection limit. Nevertheless rough results have been processed considering diffusion and photochemistry. It has only been possible to quantify the 147 nm irradiations results.
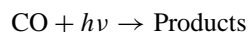
$$\text{CO} + h\nu \rightarrow \text{Products}$$

Products are CO_2, C_3O_2 [17] with $\sigma_{147\,\text{nm}}=2\times10^{-18}\,\text{cm}^2$ [17], $\Phi=1$ to calculate $J=6\times10^{-3}\,\text{s}^{-1}$, $s_{\text{CO}}=0.37\,\text{nm}$ [29] to calculate $D_{\text{CO}/\text{He}}\sim350.4\,\text{cm}^2\,\text{s}^{-1}$. As the residence time is also $\tau\sim4\,\text{s}$, photodestruction of CO is about 3% of its production from POM, which is not significant compared to the dispersion of our results. Nevertheless, formaldehyde photochemistry contribute to CO production according to the following processes [17]:
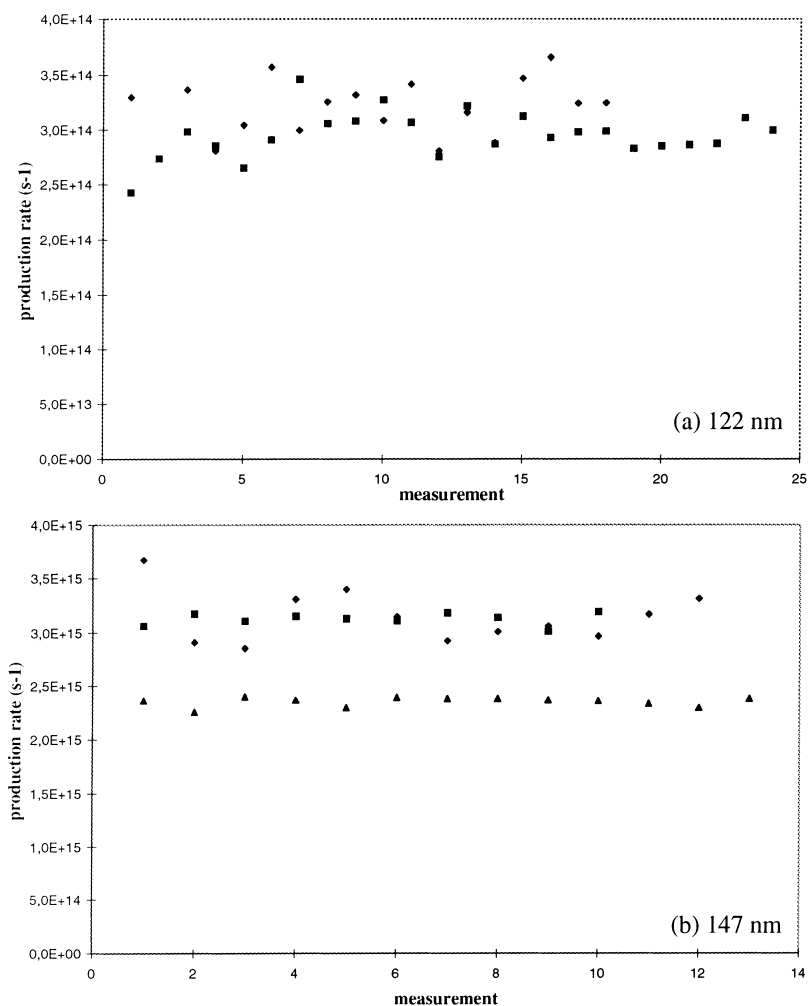
Fig. 6. Production rate of formic acid from POM. (a) For two independent irradiation experiments at 122 nm; (b) three independent experiments at 147 nm.
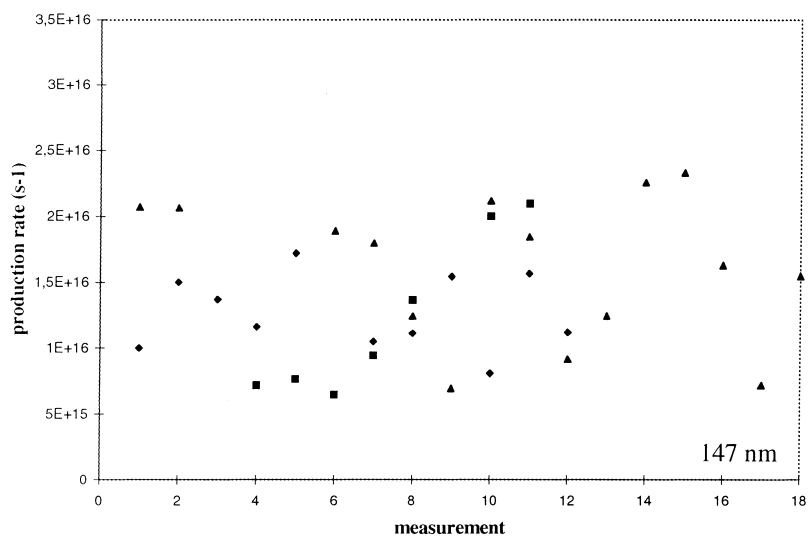

Fig. 7. Production rate of carbon monoxyde from POM for three independent experiments at 147 nm.

Table 1
Results obtained for each wavelength and molecule

Molecule/λ (nm)	122	147	193
H_2CO	0.75±0.21	0.96±0.19	<0.16
HCOOH	0.13±0.05	0.26±0.10	ε
CO	Not estimated	~1	ε
CO_2	Not estimated	~0.3	ε
CH_3OH	~0.05	~0.05	ε

$$H_2CO + h\nu \rightarrow CO + H_2$$

$$H_2CO + h\nu \rightarrow CO + 2H$$

$$H_2CO + h\nu \rightarrow HCO + H$$

$$H + HCO \rightarrow H_2 + CO$$
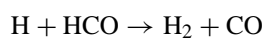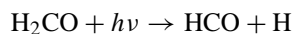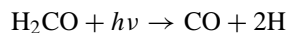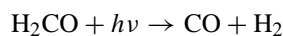
$$2HCO \rightarrow 2CO + H_2$$
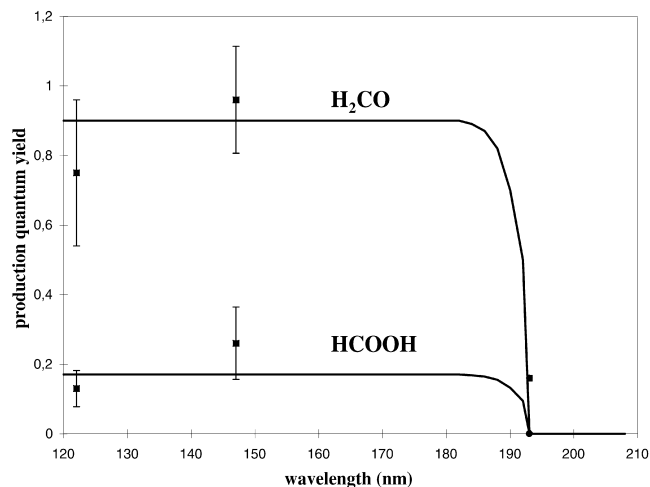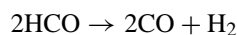
Fig. 8. Quantum yield profiles as a function of the wavelength for H_2CO and HCOOH according to our experimental measurements.
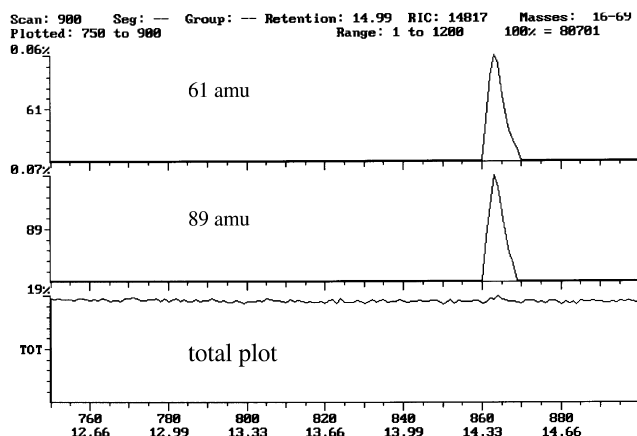

Fig. 10. Evidence of the presence of trioxane from its characteristic mass fragments at 61 and 89 amu.

Considering this chemical system, a production quantum yield of CO from H_2CO of 1 is assumed. Then, net production of CO from POM is $V_{CO/147\,nm}=1.42\times10^{16}\pm1.05\times10^{16}\,s^{-1}$, i.e. 74% of relative uncertainty. Finally: $Q_{CO/147\,nm}=1.3\pm0.9$.

Such a result, in spite of the large uncertainty, is important because it shows that productions of H_2CO and CO by photodegradation of POM have the same order of magnitude. It rises the new idea that POM may also directly contribute to the extended source of CO in comets.

3.4.3. CO_2

An important experimental difficulty is encountered for the quantification of CO_2, because of its presence (as an atmospheric compound) in the compartment between the simulation chamber and the infrared spectrometer. In spite of a continuous nitrogen purge, we were not able to maintain its concentration in the compartment at a constant level during experiments of 5 to 8 h. Nevertheless, the evolution of this concentration has been studied before starting an irradi-
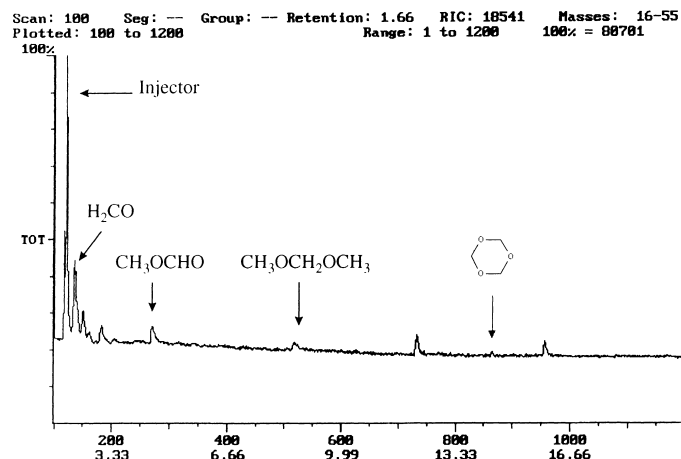

Fig. 9. Chromatogram of the photodegradation products of POM after concentration in a cold trap.

Fig. 11. Chemical mechanisms involved in the photodegradation of polyoxymethylene.

ation at 147 nm. By extrapolation during the experiment, a rough estimation of its production rate by photodegradation of POM is possible. Quantification has been made with the 667 cm^{-1} band surface referring to a calibrated spectrum at atmospheric pressure. Experimentally, we have calculated that, for the same amount of CO_2, the surface ratio of the 614 cm^{-1} band, between atmospheric pressure and the 2 mb

of total pressure at which our irradiation experiments are performed, is 7 (saturation at low pressure). This method yields $Q_{CO_2/147\,nm} \approx 0.3$.

3.4.4. CH_3OH

The concentration of methanol is generally too small to be measured with accuracy. Thus results are very scattered

and allow only a rough estimation of its quantum yield at 122 and 147 nm

$$Q_{CH_3OH/122\,nm\,\&\,147\,nm} \approx 0.05$$

3.4.5. Sum-up

Results obtained for each wavelength and molecule are summarized in Table 1.

By extension, for H_2CO and $HCCOH$, we propose to adopt profiles presented on Fig. 8.

3.4.6. GC-MS analysis

A typical chromatogram obtained after concentration of photodegradation products in a cold trap is shown on Fig. 9. Designated compounds have been identified from their mass spectrum and retention time of their peaks measured after injection of the pure compound. We have detected H_2CO, CH_3CHO, $CH_3OCH_2OCH_3$ (dimethoxymethane) and $C_3O_3H_6$ (trioxane). Trioxane peak is almost in the noise of the total mass chromatogram, but its detection is obvious when its characteristic masses 61 and 89 amu are specifically followed (Fig. 10). Furthermore, the later have the retention time that has been measured during calibration of pure trioxane in our experimental conditions. CO was not detected because it is not trapped in liquid nitrogen. The peak of the CO_2 produced in the experiment elutes together with the peak produced by the action of the gas injector into the column (operated by compressed CO_2). HCOOH and CH_3OH are not eluted on this column. Some peaks have not been identified, but according to the structure of the polymer and the identified photofragments, we can suspect the presence of molecules such as: CH_3OCH_3, CH_3CHO, CH_3OCH_2CHO, CH_3OCH_2OH.

3.5. Chemical mechanisms

Contrary to the statement formulated in Rabek [2], formaldehyde is not the only photodegradation product of polyoxymethylene. The diversity of products we observe is close to the results presented in Fischer and Langbein by radiolysis [16] and quoted in our introduction. On Fig. 11, chemical mechanisms leading to the formation of all our detected compounds are proposed. Initiation, termination, copolymerization steps, and H_2CO production are from ref [2,16]. CO and CO_2 productions have been drawn from Roessler et al. [15], but we have corrected mechanisms and reactions formalism to be conform with polymer chemistry customs. For other products, we present new mechanisms inspired from chemistry involved during polymers photodegradation as described in textbooks on that topic [2,32]. An important step for the production of CO, CO_2, HCOOH and CH_3OCHO, is the formation of a carbonyl group in the polymer chain by combination of two adjacent radicals.

Quantum yields measured in this study are the result of a complex competition between initiation, production and termination reactions, rather than a simple reaction such as: one photon produces one molecule.

4. Conclusion

In the frame of the cometary organic chemistry study and particularly the preparation of the European Space Agency ROSETTA mission, we have developed an experimental setup to study the photodegradation of high molecular weight compounds in the vacuum UV. We have identified the main gaseous degradation products of polyoxymethylene by photodegradation, and calculated production quantum yields for some of them. Such data were missing to interpret astronomical observations of a molecule like H_2CO in comets and are now available for further theoretical studies. This work is followed out into three directions:

- The study of other molecules to obtain fundamental physico-chemical data about their photodegradation. Candidate compounds for such studies applied to comets are hexamethylenetetramine: $C_6H_{12}N_4$, HCN polymers, polycyclic aromatic hydrocarbons and amino acids. Thermal regulation of our reactor allows us also to study thermal degradation of these compounds.
- Astronomical observations of molecules like dimethoxymethane and trioxane that haven't yet been detected in comets and should be observed if POM is present.
- Theoretical simulations of the behavior of POM in cometary atmospheres to answer to which extend its presence could explain the observed formaldehyde extended source. Publication of first applications of this study for comet Halley is in preparation (Cottin et al., in preparation).

Our experimental development and results, as described above, have direct astrophysical applications, but may also provide fundamental parameters, such as quantum yields of production of gaseous compounds, concerning photodegradation of any molecule in the solid state. Furthermore, the identification of photofragments provides important clues about mechanisms involved during the photodegradation.

Acknowledgements

References

[1] S.W. Shalaby, J. Polym. Sci.: Macromol. Rev. 14 (1979) 419–458.
[2] J.F. Rabek, Polymer Photodegradation: Mechanisms and Experimental Methods, Chapman & Hall, London, 1995.

[3] J. Crovisier, Faraday Discussion 109 (1998) 437–457.

[4] H. Cottin, M.C. Gazeau, F. Raulin, Planetary Space Sci. 47 (1999) 1141–1162.

[5] P. Eberhardt, D. Krankowsky, W. Schulte, U. Dolder, P. Lammerzahl, J.J. Berthelier, J. Woweries, U. Stubbeman, R.R. Hodges, J.H. Hoffman, J.M. Illiano, Astronomy Astrophys. 187 (1987) 481–484.

[6] M.A. DiSanti, M.J. Mumma, N.R.D. Russo, K. Magee-Sauer, R. Novak, T.W. Rettig, M.N. Fomenkova, Bull. Am. Astronomical Soc. 29 (1997) 34–102.

[7] M.A. DiSanti, M.J. Mumma, N. DelloRusso, K. Magee-Sauer, R. Novak, T.W. Rettig, Nature 399 (1999) 662–665.

[8] R. Meier, P. Eberhardt, D. Krankowsky, R.R. Hodges, Astronomy Astrophys. 277 (1993) 677–691.

[9] N. Biver, D. Bockelée-Morvan, J. Crovisier, J.K. Davies, H.E. Matthews, J.E. Wink, H. Rauer, P. Colom, W.R.F. Dent, D. Despois, R. Moreno, G. Paubert, D. Jewitt, M. Senay, Astronomical J. 118 (1999) 1850–1872.

[10] D. Bockelée-Morvan, J. Wink, D. Despois, N. Biver, P. Colom, J. Crovisier, E. Gerard, E. Lellouch, L. Jorda, Bull. Am. Astronomical Soc., 30, 1998, 31.02.

[11] W.F. Huebner, D.C. Boice, A. Korth, Adv. Space Res. 9 (1989) 29–34.

[12] W.A. Schutte, L.J. Allamandola, S.A. Sandford, Icarus 104 (1993) 118–137.

[13] N. Biver, Doctorat, Université Paris VII, 1997.

[14] J.M. Greenberg, A. Li, Astronomy Astrophys. 332 (1998) 374–384.

[15] K. Roessler, M. Sauer, R. Schulz, Ann. Geophys. 10 (1992) 226–231.

[16] V.H. Fischer, W. Langbein, Kolloid-Zeitschrift und Zeitschrift für Polymere 216–217 (1967) 329–336.

[17] H. Okabe, Photochemistry of Small Molecules, Wiley-Interscience, 1978.

[18] H. Cottin, Thèse de Doctorat, Université Paris XII, Créteil, 1999, http://www.lisa.univ-paris12.fr/GPCOS/Hc/H1t.htm

[19] T.G. Slanger, G. Black, J. Chem. Phys. 68 (1978) 1844–1849.

[20] H.J. Kuhn, S.E. Braslavsky, R. Schmidt, Pure Appl. Chem. 61 (1989) 187–210.

[21] N.R. Greiner, J. Chem. Phys. 47 (1967) 4373–4377.

[22] N.S. Smith, F. Raulin, J. Photochem. Photobiol. 124 (1999) 101–112.

[23] M. Zelikoff, K. Watanabe, J. Opt. Soc. Am. 43 (1953) 756–759.

[24] H. Cottin, M.C. Gazeau, J.F. Doussin, F. Raulin, Phys. Chem. Earth 24C (1999) 597–602.

[25] J.F. Doussin, D. Ritz, R.D. Jolibois, A. Monod, P. Carlier, Analusis 25 (1997) 236–242.

[26] J.F. Doussin, D. Ritz, P. Carlier, Appl. Opt. 38 (1999) 4145–4150.

[27] M. Suto, X. Wang, L.C. Lee, J. Chem. Phys. 85 (1986) 4228–4233.

[28] M. Dobrijevic, Thése de Doctorat, Université Bordeaux I, 1996.

[29] R.C. Reid, J.M. Prausnitz, B.E. Poling, The Properties of Gases and Liquids, 4th Edition, McGraw-Hill, New York, 1987.

[30] F.S. Dainton, K.J. Ivin, D.A.G. Walmsley, Trans. Faraday. Soc. 55 (1959) 61–64.

[31] M. Suto, X. Wang, L.C. Lee, J. Phys. Chem. 92 (1988) 3764–3768.

[32] J.F. Rabek, Photodegradation of Polymers: Physical Characteristics and Applications, Springer, 1996.